British Journal of Applied Science & Technology
16(3): 1-14, 2016, Article no.BJAST.26663
ISSN: 2231-0843, NLM ID: 101664541

SCIENCEDOMAIN *international*
www.sciencedomain.org

In-Plane Shear Properties of Nano-Hybridized GFRE Composites with MWCNTs

S. M. Aldousari[1*]

[1]Department of Mechanical Engineering, Faculty of Engineering, King Abdulaziz University, P.O.Box 80204, Jeddah 21589, Saudi Arabia.

Author's contribution

The sole author designed, analyzed and interpreted and prepared the manuscript.

Article Information

DOI: 10.9734/BJAST/2016/26663
Editor(s):
(1) Manoj Gupta, Department of Mechanical Engineering, NUS, 9 Engineering Drive 1, Singapore 117576, Singapore.
Reviewers:
(1) Bhagwan F. Jogi, Dr. B.A. Technological University, India.
(2) Matheus Poletto, Universidade de Caxias do Sul, Brazil.
Complete Peer review History: http://sciencedomain.org/review-history/14818

Original Research Article

Received 27th April 2016
Accepted 26th May 2016
Published 30th May 2016

ABSTRACT

Epoxy resin modified with nanofillers cannot be used alone for high performance structural applications due to their low-mechanical properties. Therefore, the main objective of this work is to hybridize composite laminates with different fiber configurations by 1.0 wt% multi–walled carbon nanotubes (MWCNTs). The hybridized composite laminates include, quasi-isotropic $[0/\pm45/90]_s$ glass fiber reinforced nanophased-epoxy (QI-GFR/MWCNT/E) and unidirectional $[0]_8$ UD-GFR/MWCNT/E. In parallel, control laminates are fabricated without MWCNTs. Results from Iosipescu shear characterization showed that the in-plane shear (IPS) strength and modulus of MWCNTs-nanocomposite are improved by 40.9% and 21.9% respectively compared to neat epoxy. The IPS strengths of QI-GFR/MWCNT/E and UD-GFR/MWCNT/E laminates are improved by 39.5% and 1.4% respectively. The IPS moduli of the hybridized composite laminates showed about 17% improvement compared to the control laminates. The improvement in the IPS properties of the hybridized composite laminates was due to the good interface bond strength between the constituent materials. The predicted IPS modulus of MWCNT/E using Halpin-Tsai model agrees very well with the experimental results with only 4.2% variation.

**Corresponding author: E-mail: saadaldousari570@yahoo.com, sdossary@kau.edu.sa;*

Keywords: MWCNT; nanocomposites; nano-hybrid glass fiber composites; in-plane shear; ultrasonics.

1. INTRODUCTION

This study is a continuation of previous work, introduced in [1-3] on the tensile, compression, flexural and damping properties of MWCNT/E nanocomposites and nano-hybridized fiber reinforced composite laminates.

In recent years, major advances in automotive and aerospace industries have motivated researchers to work on new structural materials possessing high specific properties. Although, carbon nanotube (CNT) reinforced polymer nanocomposites are one of the advanced materials showing a multitude of attractive mechanical, thermal, chemical, electrical and optical characteristics it cannot be used as structural application due to their lower mechanical properties compared to the advanced fiber reinforced polymer (FRP) composites. Therefore, one of the objectives of the present study is to hybridize the advanced FRP composites with multi-walled carbon nanotubes (MWCNTs).

Carbon nanotubes (CNTs) are known to have an elastic modulus of up to 1 TPa and predicted tensile strengths of the order of 100 GPa [4]. The interfacial bond strength between epoxy and CTs plays a very important role in determining the different properties of composite materials. A strong interfacial bond results in composites with high strength and stiffness owing to transferring the load from the lower strength matrix to higher strength CNTs. One of the important parameter that limits the interface bond is the dispersion of CNTs in epoxy resin. Due to the high–surface energy of nanotubes they have a tendency to aggregate together owing to the strong attractive forces between the CNTs themselves. The van der Waals attractive interactions owing to high aspect ratio of MWCNTs are another reason for the agglomeration of CNTs in epoxy resins [5-13]. The aggregated CNTs are in the form of bundles or ropes [11], usually with highly entangled network structure that is very difficult to disperse them. Therefore, the homogeneous dispersion of nanofillers within the polymer matrix is a prerequisite of any composites and verified remain problems to be solved. In the present work, special attention will be paid to select the best sonication parameters for dispersion MWCNTs in epoxy resin.

The epoxy monomers react with curing agent (generally containing amine groups) during its cure to form a three–dimensional cross–linked network with a certain thermomechanical properties. The degree and uniformity of curing reaction will affect considerably the bulk material properties [14]. Various degrees of CNT concentrations may influence curing reactions to a different degree or sometimes with opposite effect [15]. Zhou et al. [16] showed that both unfunctionalized and functionalized multi–walled carbon nanotubes (MWCNTs) have an accelerating influence on the reaction kinetics. They also found that the degree of epoxy cure is decreased by the addition of 1 wt% unfunctionlized MWCNTs. This result was evidenced by the lower value of the glass transition temperature (T_g) of the cured nanocomposite by 15℃ compared to the neat epoxy. Tao et al. [17] also observed that with only 1 wt % of carbon nanotubes, the T_g of epoxy composites was lowered by 10–30℃ approximately. As discussed above, the effects of CNTs on the curing reaction can lead to significant thermal and mechanical property changes of CNT/epoxy nanocomposites, which would complicate their property evaluation. This issue has attracted more and more attention recently, but only limited progress has been made. This is likely due to the difficulty in the quantitative assessment of the above effect [15].

There are many mechanical tests, which can be used to characterize the strength of the interfacial bond [18]. The most common are the single fiber pullout/microdrop technique, the embedded single fiber test and the microdebonding/microindentation technique. For bulk composites, there are the short beam shear test, the transverse tensile test, the transverse flexural test and the Iosipescu shear test. Compared with other test methods, such as the thin-walled tube torsion test and the solid rod torsion test, the V-notch Iosipescu shear test uses a flat specimen that is easier to fabricate while achieving a pure and uniform shear stress–strain state over the test region. Consequently, more reliable results can be obtained, and the test has become well accepted among researchers in the field [19]. Accordingly, Iosipescu shear test will be used in the present work to characterize the newly developed materials.

Tsai and Wu [20] characterized the interfacial bond strength using in-plane shear tests, transverse tensile tests, and the transverse flexural tests of the organoclay GFE composites. The IPS properties were determined using $[\pm 45]_s$ tension and the interlaminar fracture toughness was measured using double cantilever beam (DCB). In these tests the composite properties are controlled by the matrix. Their results showed that IPS strength, transverse flexural strength and transverse tensile strength are improved with the increase of the organoclay (2.5 to 7.5 wt%). In contrast, the longitudinal tensile strength and the interlaminar fracture toughness of the fabricated GFE nanocomposites decreases as the organoclay loading increases. For the matrix modified with the organoclay, the corresponding mechanical properties become brittle so that the plastic zone around the crack tip is small, allowing the crack to extend easily. As a result, the presence of organoclay has a negative effect on the interlaminar fracture toughness of the fiber reinforced nanocomposites.

Kim et al. [21] showed that the in-plane shear (IPS) modulus of CNT/E nanocomposites with 0.3 wt% was improvement by 8.82% compared to neat epoxy. The IPS modulus of the hybridized fabric CFR/CNT/E laminates was also enhanced by 8.1%, as the CNTs reinforce the inter-filament epoxy matrix in the composite strand against shear in the longitudinal direction.

This research aims to perform a symmetric investigation regarding the multiwall carbon nanotube (MWCNT) effect on the mechanical properties of different composite configurations. Nanophased epoxy is ultrasonically prepared and used to fabricate epoxy/MWCNT nanocomposite as well as to hybridize advanced composite laminates with different fiber configuration. The hybridized composite laminates include, quasi-isotropic $[0/\pm 45/90]_s$ glass fiber reinforced nanophased-epoxy (QI-GFR/E/MWCNT) and unidirectional $[0]_8$ glass fiber reinforced nanophased-epoxy (UD-GFR/E/MWCNT). The dispersion of 1.0 wt% MWCNT in epoxy resin is carried out using high intensity ultrasonic liquid processor. The composite laminates (with and without MWCNT) are locally fabricated using hand lay–up technique. Special roller is applied with moderate pressure for remove any visible air bubbles, provides fast impregnation and good wetting of glass fibers with wetting fiber and de–agglomerations of MWCNTs in composite laminates. The in-plane shear properties (strengths and moduli) are determined via Iosipescu shear tests.

2. EXPERIMENTAL WORK

2.1 Materials

Six different materials categories are prepared in this work. Three of them includes MWCNT in their compositions which are MWCNT/epoxy nanocomposites, quasi–isotropic $[0/\pm 45/90]_s$ glass fiber/MWCNT/epoxy composite laminate (QI–GFR/MWCNT/E), unidirectional glass fiber/MWCNT/epoxy composite laminate (UD–GFR/MWCNT/E). In parallel, three control panels without MWCNTs in their composition are fabricated. The selected percent of MWCNT is 1.0 wt%, which has showed improvement in the mechanical properties by many investigators [1-3,8,17,22-26]. Details about the constituent materials of the present work are presented in Table 1.

2.2 Fabrication of the Neat Epoxy (NE), MWCNTs-composites

Details about the fabrication procedure of neat epoxy (NE), MWCNTs-nanocomposites and the nano-hybrid GFRP composites were described earlier by Aldosari et al. [1-3] as shown in the next sections.

2.2.1 Preparation of neat epoxy panel

Epoxy part A (100 part by weight) was mixed with epoxy part B (45 part by weight) and stirred manually for 10 min [23]. The hardener (epoxy part B) was added gradually (i.e. drop by drop) while the mixture was being stirred. After stirring the epoxy resin was poured into glass mold (300 mm x 300 mm) that was treated by release agent (liquid wax). The mold then precured in an oven for 4 h at a temperature of 40℃ and post cured by ramping the temperature from 40℃ to 80℃ and hold for 2 h [27].

2.2.2 Preparation of MWCNT/E nano-composites

In the present work 1 wt% of MWCNTs was dispersed in epoxy resin using a high intensity Ultrasonic Processor, Cole–Parmer, Inc., USA. The dispersion of MWCNTs is more difficult in a viscous medium, where the viscosity of polymer increased sharply as the CNTs loading increased [28]. Due to the fact that sonication parameters

can play an important role in enhancement the dispersion of CNTs in viscous polymers and accordingly the mechanical properties of the nanocomposites, the following sonication parameters are carefully selected based on the literature review to disperse MWCNTs in epoxy part A:

- To overcome the temperature raise during sonication process a cylindrical aluminum containers with flat bottom and small diameter (80 mm) is immersed in ice cooling bath to a level roughly equal to that of the internal mixture. The high thermal conductivities of the aluminum will maximize the dissipation of heat by the water/ice cooling bath. The small diameter of the container will maximize the surface area of the mixture that is subjected to the water/ice cooling bath and consequently the dissipation of heat by the cooling bath. In addition, the small diameter of the container will maximize the mixture–probe surface area exposed to the acoustic waves.
- Sonicator probe with 25 mm diameter was fixed for all the sonication processes [28]. Probes with larger tip diameters produce less intensity, but the energy is released over a greater area. The larger the tip diameter, the larger the volume that can be processed, but at lower intensity.
- Immersion depth of the sonicator probe was fixed at 50 mm, at the center of the container (to avoid the contact between the probe and the container walls), and away about 20 mm from the bottom of the container. Probe immersion depths between (20 to 50 mm) are recommended to prevent the nebulization (formation and release of aerosols) owing to rise of agitation surface [29].
- The maximum sonication temperature did not exceed 70℃ [30]. For this purpose, temperature probe tip was fixed at about 1 cm away from the sonicator probe [29].
- Another important parameter for the ultrasonic dispersion is the sonication amplitude, which is correlated to the power input into the mixture. The maximum sonication amplitude (100%) was applied during the sonication processes. It has been addressed that the best dispersion results are obtained at the highest amplitude of 100%, and hence the highest power input [31,32].
- Constant sonication energy (2700 kW.s). The increased viscosity of the epoxy resin due to mixing MWCNTs can dampen the cavitation process. Therefore, sonication power of 750 W was applied for 60 min [5].
- Constant energy densities (7714 W·s/ml). All the sonication processes were implemented at constant energy densities using constant mixture volume 350 ml. Bittmann et al. [31] reported that the time needed to achieve a good dispersion of TiO_2 nanoparticles/epoxy is approximately proportional to the mixture volumes.
- Operating in pulsed mode with 15 s on and 30 s off. Sonication in pulsed mode retards the rate of temperature increase in the mixture, minimizing unwanted side effects and allowing better temperature control than continuous mode operation. Pulse mode operation with long off periods will help avoid foaming in samples [29]. Uddin and Sun [28] applied 15 s on and 15 s off, while Chen et al. [32] applied 12 s on and 48 s off. On the other hand Zhou et al. [33] applied 50 s on and 25 s off.

After dispersing the MWCNTs in epoxy resin, the hardener (epoxy part B) was added to the mixture and manually stirred for 10 min [23]. The nanophased–epoxy now is ready to pour into the mold and/or to hybridize the glass fiber composite laminates. For MWCNT/E nanocomposites, the panels were prepared and cured by following the same manufacturing procedure of the neat epoxy panel.

2.2.3 Fabrication of hybrid multi–scale GFR/MWCNT/E composite laminates

Two types of hybrid multi–scale GFR/MWCNT/E composite laminates are fabricated using hand lay–up technique. The first type is the QI–GFR/MWCNT/E laminate and the second type is UD–GFR/MWCNT/E laminate. The fabrication procedure is shown in the following section.

(a) Fabrication of QI–GFR/MWCNT/E composite laminates

- Eight templates were used to lay–up the fiber bundles in 0°, +45° –45°, 90°, 90°,–45°,+45°, and 0° directions. The parallel bundles of fibers were fixed on the frame of the templates. The normal distance between the adjacent bundles was five mm.

- The upper surface of the mold is glass plate (600x400 mm) treated by release agent (liquid wax).
- The first layer of the nanophased epoxy resin was spread on the glass plate.
- The first template with glass fiber in 0° direction was placed on the nanophased epoxy and consolidated using aluminum roller with longitudinally narrow slots parallel to its axis and perpendicular to the fiber directions. This type of rollers removed any visible air bubbles that escaped into the slots and provides fast impregnation and good wetting of glass fibers with the nanophased matrix. In additions, applying rolling with moderate pressure can play an important role in de–agglomeration of the MWCNTs owing to the strong attractive forces between the CNTs themselves and the van der Waals attractive interactions arise from the high aspect ratio of MWCNTs. Therefore, the resultant laminate has good fiber–matrix interfacial bond strength.
- Rolling is continued until the lamina is fully impregnated and all visible air inclusions are removed which observed by the eyes. This procedure was repeated with alternative layers of nanophased epoxy and the next glass fiber layers, which are in the following sequence: 0°, +45°, –45°, 90°, 90°,–45°,+45°, and 0°.
- A cellophane paper that wounded on a smooth round aluminum pipe and rolled to remove any visible air bubbles and squeeze the excess resin covered the last layer (nanophased epoxy).
- To obtain smooth upper surface with nearly constant thickness a glass plate was placed on the cellophane paper and a weight of 30 kg was distributed on it, BS 3496.
- The laminate was precured under uniform pressure for 24 h at room temperature, ISO 1268, and post cured at room temperature for further 21 days.
- The margins of the laminate, up to at least 20 mm from the edge, were cut and the working portion of the specimens was taken away from the edge by about 30 mm.

Table 1. Constituents of the investigated materials

Test materials	Material abbreviated name	Constituent materials
Neat epoxy	Neat epoxy	Epoxy part A (Resin): Araldite PY 1092–1 (100 part by weight) ρ_A = 1.15 g/cm^3. Epoxy part B (Hardener): HY 1092 (45 part by weight) ρ_B = 1.0 g/cm^3. Viscosity of epoxy (A and B) is 300 cps at 25℃.
Multi–Wall Carbon Nanotube/Epoxy nanocomposites	MWCNT/E	Epoxy MWCNT: 1 wt% (epoxy parts A+B) ◦ Outer diameter < 8 nm ◦ Length 10–30 µm ◦ Purity > 95 wt%
Quasi–isotropic $[0/\pm45/90]_s$ glass fiber reinforced epoxy composite laminates	QI–GFR/E	Epoxy E–roving glass–fiber linear density = 1.2 g/m.
Quasi–isotropic $[0/\pm45/90]_s$ glass fiber reinforced MWCNT/epoxy composite laminates	QI–GFR/ MECNT/E	Epoxy E–roving glass–fiber linear density = 1.2 g/m. MWCNT:1 wt% (epoxy parts A+B)
Unidirectional glass fiber reinforced epoxy composite laminates	UD–GFR/E	Epoxy E–roving glass–fiber linear density = 1.2 g/m.
Unidirectional Glass fiber reinforced MWCNT/epoxy composite laminates	UD–GFR/MWCNT/E	Epoxy E–roving glass–fiber linear density = 1.2 g/m. MWCNT:1 wt% (epoxy parts A+B)

The quasi–isotropic $[0/\pm45/90]_s$ angle–ply glass fiber reinforced epoxy composite laminate (QI–GFR/E) was manufactured by the same procedure using neat epoxy resin instead of nanophased epoxy resin.

(b) Fabrication of UD–GFR/MWCNT/E composite laminates

The unidirectional composite laminate UD–GFR/E and UD–GFR/MWCNT/E composite laminates were fabricated by following the same manufacturing procedure of QI–GFR/E and QI–GFR/MWCNT/E respectively using eight layers of unidirectional glass fiber.

The fiber volume fractions (V_f) of the manufactured laminates are determined experimentally using the ignition technique according to ASTMD3171. The average value of V_f is 33.7%. The variation of V_f in any laminate not exceeds ±0.1% while, the variation of V_f among the fabricated laminates (QI-GFR/E, QI-GFR/MWCNT/E, UD-GFR/E, and UD-GFR/MWCNT/E) was ±0.4% due to the different fibers configurations in these laminates.

2.3 Scanning Electron Microscopy (SEM)

The fracture surfaces of some specimens were examined using scanning electron microscope (SEM) model Nova NanoSEM–230 operating at 3 kV. The SEM specimens were cut through a collimated plane under the fractured surface by 3 mm. The specimens were bonded to metallic support using both sided carbon tape. To improve conductivity of the fracture surfaces, the specimens were deposited with a thin layer of gold using a vacuum evaporator for 5 min. It is called as gold sputtering

2.4 In-plane Iosipescu Shear Tests

In-plane shear tests are implemented on the investigated materials in accordance with ASTM D5379 using computer controlled universal testing machine model CMT5205/5305 MTS SYSTEMS. The in-plane shear loads are applied on double notch specimens using Iosipescu test fixture at constant cross-head speed of 2 mm/min. The principle of the test is to apply a state of pure shear stress [19] at the specimen mid-length through two counteracting moments produced by the force couples of the movable grip with respect to the fixed grip as shown in Fig. 1. A 90° double V-notches were machined through the thickness of 76 mm x 20 mm strips using form-milling cutter for a depth of 4 mm as shown in Fig. 2. The radius of the notch root is 1.3 mm in all the specimens.

To measure the shear strain (γ_{xy}) and shear modulus (G_{xy}) two strain gages were bonded at ±45°to the center of the test specimen as shown in Figs. 5 and 6. The strain gages are connected to PC via 4-channed data acquisition model 9237 NI.

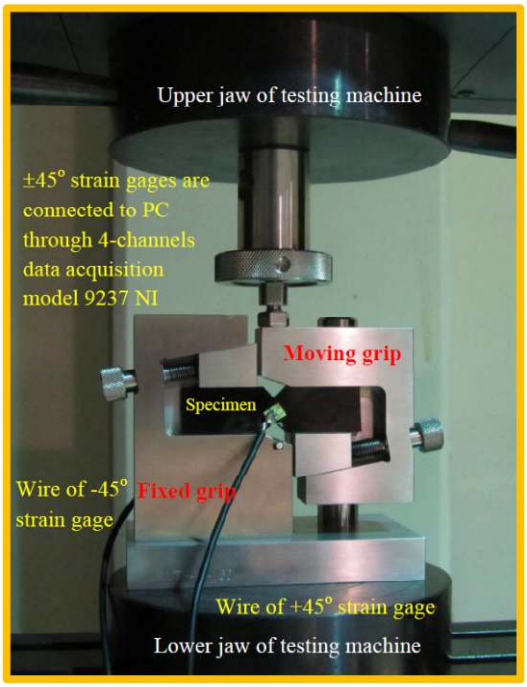

Fig. 1. Experimental setup for Iosipescu shear test

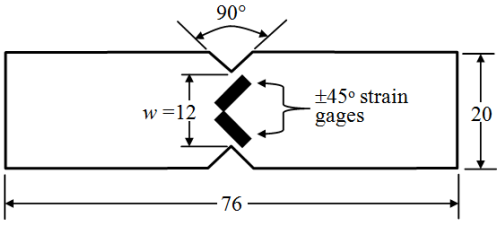

Fig. 2. Dimensions of double V-notch shear test specimen

3. RESULTS AND DISCUSSION

3.1 Dispersion of MWCNTs

During dispersion of MWCNTs in epoxy resin the sonication temperature did not exceed 70℃ due

to implementation the pulsed mode with 15 s on and 30 s off and using high thermal conductivities aluminum container surrounded by water/ice cooling bath. If the temperature reached 70℃ the feedback signal of temperature probe stopping the instrument until the temperature reduced to 68℃ then restart the sonication process. Sonication at maximum amplitude (100%) leads to raise the mixture temperature to about 70℃ that helps to overcome the increase in viscosity as a result of added MWCNTs. The sonication process develops more cavitation bubbles, which have growing during several cycles until they attain a critical diameter. The collapse of these bubbles causes locally extreme conditions as a very high local pressure and temperatures, and hence splitting up the agglomerated MWCNTs [28,31]. The shock waves from the implosive bubble collapse in combination with micro-streaming generated by cavitation oscillations lead to dispersion effects. Fig. 3 shows that the selected sonication parameters result in a good distribution of MWCNTs in epoxy resin.

3.2 Load-displacement Behavior

Figs. 4 and 5 show samples from the load-displacement curves of the investigated materials. The load-displacement curves of neat epoxy and MWCNTs-nanocomposite have nonlinear load-displacement behavior accompanied with plastic deformations at the ultimate loads as shown in Fig. 4. The plastic deformation is visually observed on the fractured specimens as shown in Fig. 6a. The MWCNTs-nanocomposite exhibits higher ultimate loads and displacements compared to the neat epoxy. This result was due to transferring the load from the matrix to the well dispersed high strength MWCNTs via the interfacial bond between them. Therefore, this result is a direct indication for the strong interface bond between MWCNTs and matrix.

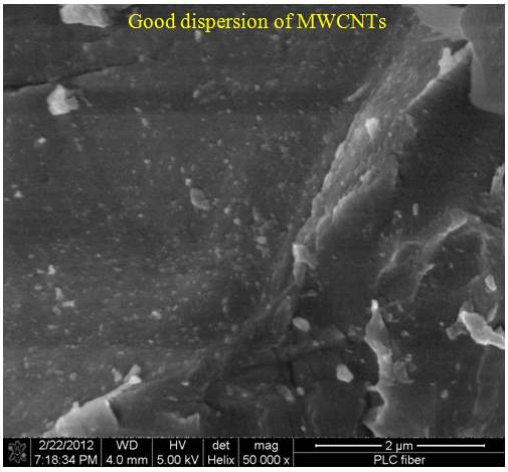

Fig. 3. SEM image of fractured MWCNTs-nanocomposite showed good dispersion of MWCNTs in epoxy resin

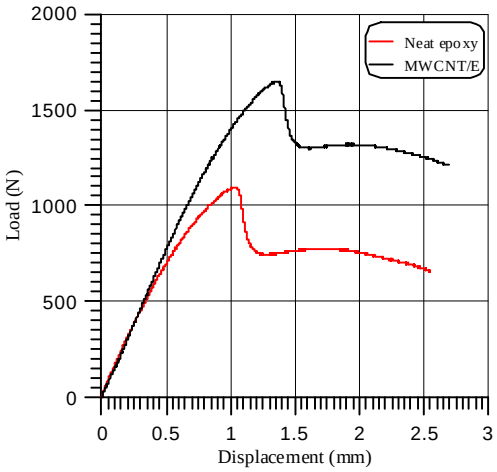

Fig. 4. Load-displacement diagrams of neat epoxy and MWCNT/E nanocomposites in shear tests

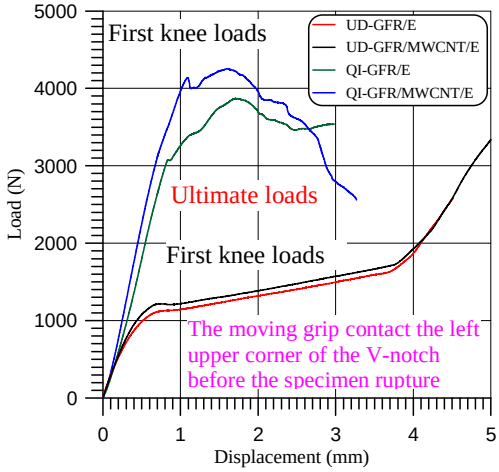

Fig. 5. Load-displacement diagrams of nano-hybridized and control laminates in shear tests

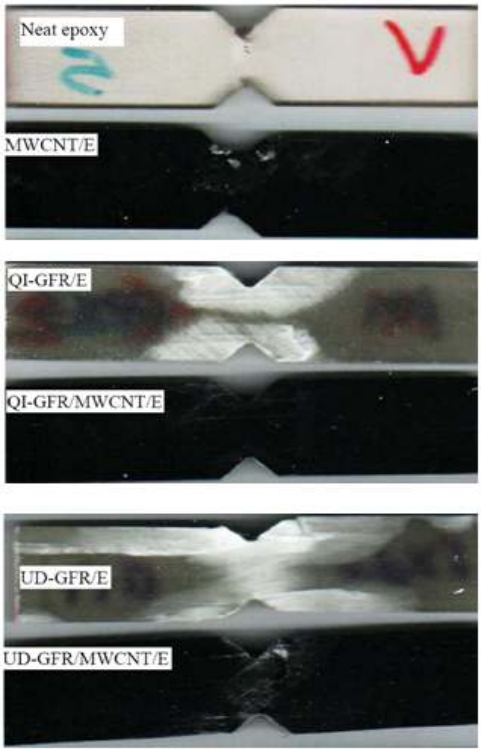

Fig. 6. Photographs of some fractured specimens in Iosipescu shear test. (a) neat epoxy and MWCNT/E, (b) QI-GFR/MWCNT/E laminate, and (c) UD-GFR/MWCNT/E laminate

Fig. 5 shows the load-displacement curves of the nano-hybridized GFR laminates and the control laminates. The load-displacement curves of the QI-GFR laminates shows a linear behavior up to about 70% of ultimate load followed by nonlinear portion up to the first knee. The visual observation of the specimens during the test indicate that the deviation from the linearity and the first knee was respectively due to matrix cracking and crack propagation ahead of the V-notches at the contacts with grips resulting in delamination between the layers as shown in Fig. 6b. The first knee load of QI-GFR/MWCNT/E laminate is higher than that of the control laminate (without MWCNTs). This is a direct indication for the strong interface bond between the nanophased epoxy and glass fiber because the delamination between the different layers is matrix-dominated. The above statement was validated via the fractured surfaces of the delaminated layers, which are examined using SEM [1]. The nanophased matrix appears firmly sticking to the fiber surface of UD-GFR/MWCNT/E laminate, as shown in Fig. 7a. On the other hand, the fracture surface of UD-GFR/E control laminates is characterized by clean fibers owing to the lower interfacial bond strength as shown in Fig. 7b. This result confirms that the interfacial bonding between the glass fiber and nanophased of epoxy UD-GFR/MWCNT/E laminate was stronger than that of the UD-GFR/E control laminate.

Developing crack between the roots of the V-notches required higher loads. Therefore, the load is further increased from the first knee load to the ultimate load as shown in Fig. 5. The ultimate load of QI-GFR/MWCNT/E laminate is higher than that of the control laminate owing to the improvement in the interfacial bond strength of the modified matrix (MWCNT/E).

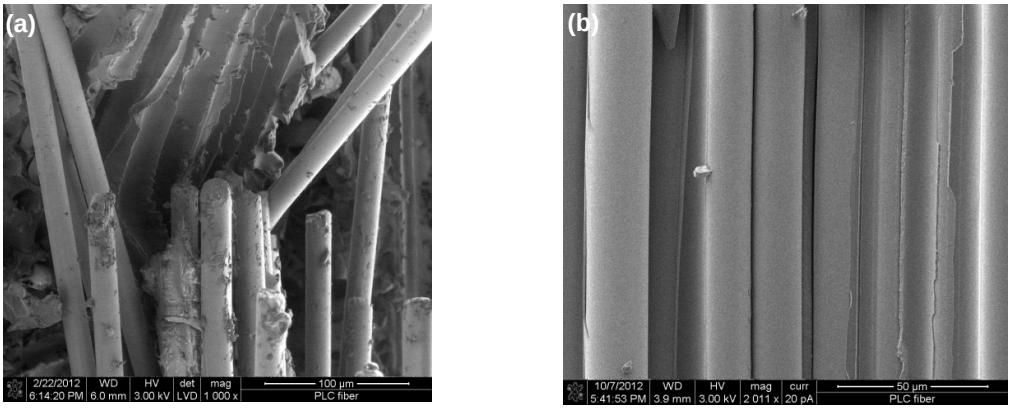

Fig. 7. SEM images of fractured surface of unidirectional laminates: (a) UD-GFR/MWCNT/E laminate, and (b) UD-GFR/E laminate

The load-displacement diagrams of UD-GFR laminates show nonlinear behavior up to the first knee load owing to matrix cracking between the roots of two V-notches that was observed visually as shown in Fig. 6c. Therefore, the stiffness of the specimen was reduced resulting in large displacements associated with small load increments up to the moving grip contact the left upper corner of the specimen V-notch. Therefore, the load is drastically increased without complete rupture of the area between the roots of two V-notches. In such case, the first knee load at which the notch root crack developed is used to calculate the shear strength as recommended by ASTM D5379. The hybridized UD-GFR laminate and the control laminate have identical qualitative load-displacement behavior. The former laminate has insignificant increase in the load values compared to the latter one because the properties of UD-GFR laminates are fiber-dominated.

3.3 In-plane Shear Strengths (IPSS)

The in-plane shear strength was calculated from the following equation:

$$\tau_{xy} = \frac{P}{A} \quad (1)$$

where *A* is the cross-sectional area between the roots of two V-notches, and *P* is the ultimate load for NE and MWCNTs-nanocomposites or the first knee load for nano-hybrid GFR/MWCNT/E composites as shown in Figs. 4 and 5 respectively.

The calculated values of IPSS for the investigated materials are presented in Table 2. The results in Table 2 and Fig. 8 indicate that the ultimate IPSS of MWCNTs-nanocomposite and the first knee IPSS of QI-GFR/MWCNT/E laminate have respectively 40.9% and 39.5% improvements compared to control panels, which did not include MWCNTs in their composition. The high improvement in IPSS of MWCNTs-nanocomposite was due to transferring the load (stress) from the matrix with lower strength to the MWCNTs with higher strength through the good interface bond strength between them.

As mentioned before, the first knee load of QI-GFR/MWCNT/E laminate was characterized by the delamination of the eight layers at the contact with loading grips. Because the delamination is a matrix-dominated, the improvement in the first knee IPSS (39.5%) approaching the same improvement level of MWCNT/E (40.9%). The good interface bond strength between the nanophased epoxy and glass fibers, Fig.7a, is another reason for the higher improvement in the first knee IPS of QI-GFR/MWCNT/E laminate compared to the control laminate. On the other hand, the ultimate IPSS of QI-GFR/MWCNT/E laminates is dominated by the ultimate failure of the different layers. The longitudinal layers with 0^o fibers are fiber-dominated and hence, their contribution to the ultimate IPSS improvements is insignificant. Accordingly, the improvement in the ultimate IPSS of QI-GFR/MWCNT/E laminate is only due to $90°$ and $\pm 45°$ layers (6-layers), which are dominated respectively by matrix and fiber/matrix interface properties. This result may interpret the lower improvement of ultimate IPSS of QI-GFR/MWCNT/E laminates (29.7%) compared to the improvement of first knee IPSS (39.5%).

The results in Table 2 and Fig. 8 also showed that the IPSS of UD-GFR/MWCNT/E laminate has insignificant improvement (1.4%). These result because the IPSS of the unidirectional laminate is controlled by the fiber properties.

Table 2. Shear properties of the investigated materials

Material	In-plane shear properties				
	τ_{xy} at1st Knee (MPa)	Std. Dev.	τ_{xy} ULT. (MPa)	Std. Dev.	G_{xy} (GPa)
Neat–epoxy	---	---	23.229	4.015	0.936
MWCNT/E	---	---	32.721	7.626	1.141
QI–GFR/E	59.396	5.027	64.963	4.278	5.204
QI–GFR/MWCNT/E	82.882	7.197	84.269	7.004	6.108
UD–GFR/E	32.959	4.991	---	---	2.339
UD–GFR/MWCNT/E	33.425	2.690	---	---	2.730

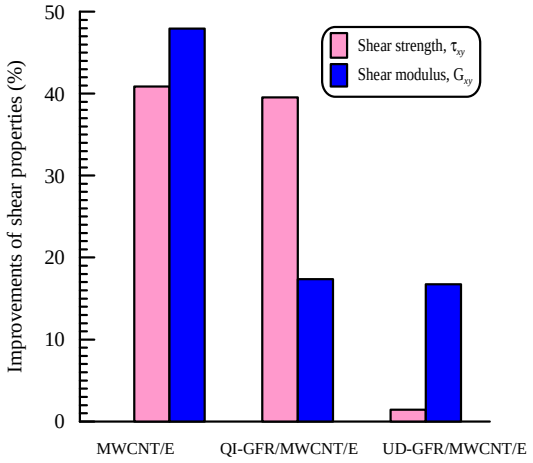

Fig. 8. Improvements of in-plane shear properties of MWCNT/E nanocomposites and nano-hybridized laminates

3.4 In-plane Shear Moduli (IPSM)

Fig. 9 shows the shear stress-strain curves of neat epoxy and MWCNT/E nanocomposites. The shear stress values are obtained from the load-displacement curves in Fig. 4 by dividing the load by the cross-sectional area between the roots of two V-notches. The strains in Fig. 9 are the measured values using ±45° strain gages. The results in Fig. 9 show that at any stress value the strains of MWCNTs-nanocomposite are lower than that for neat epoxy. This result indicates that the load (stress) in the MWCNT/E nanocomposites transferred from the matrix to the high stiffness MWCNTs through the strong interfacial bond between them, and accordingly the strain is reduced. Similar behavior was observed for the nano-hybridized GFR composite laminates as shown in Fig. 10. The results in Fig. 10 indicate that the load (stress) in the nano-hybridized GFR composite laminates transferred from the matrix to MWCNTs and glass fibers through the strong interfacial bond between them and accordingly, the strain is reduced.

The results strains (ε) of ±45° strain gages in Figs. 9 and 10 are used to calculate the in-plane shear strain (γ_{xy}) at each value of shear stress using the following equation [19]:

$$\gamma_{12} = \varepsilon_{-45} - \varepsilon_{+45} \tag{2}$$

where ε_{+45} and ε_{-45} are the measured strains of the +45° and -45° strain gages respectively.

Accordingly, the shear stress-strain curves of the investigated materials are constructed as shown in Figs. 11 and 12.

The in-plane shear moduli (IPSM) are determined from the slope of the initial linear portion of shear stress-shear strain curves ($\Delta\tau_{xy}/\Delta\gamma_{xy}$) as shown in Fig. 11 using the following equation:

$$G_{xy} = \frac{\Delta\tau_{xy}}{\Delta\gamma_{xy}} \tag{3}$$

Table 2 shows the calculated values of the IPSM of the investigated materials. The results in Table 2 and Fig. 8 showed that the IPSM of MWCNTs-nanocomposite improved by 21.9% compared to the neat epoxy. This result is due to transferring the load (stress) from the matrix with lower Young's modulus (2.247 GPa [1]) to the MWCNTs with higher Young's modulus (1 TPa [4]) through the good interface bond strength between them. The improvements in the IPSM of nano-hybridized composite laminates are about 17% compared to the control laminates as shown in Fig. 8. This result was due to the IPSM of nano-hybridized composite laminates depend on the first linear portion of the shear stress-shear strain curves, which is dominated by the enhancements in fiber/matrix properties.

3.5 Prediction the IPSM of the Investigated Materials

Voigt–Reuss has developed micromechanical model for the calculation of elastic modulus of short fiber composites, which is given below [34].

$$E = \frac{3E_L}{8} + \frac{5E_T}{8} \tag{4}$$

where E_C is the composite Young's modulus, and E_L and E_T are the longitudinal and transverse elastic modulus respectively.

Halpin-Tsai models have been used successfully to calculate the moduli (E_L and E_T) of the above equation for CNT reinforced polymer composites and the resultant equation was [5,21,34,35]:

$$E_C = E_m\left[\frac{3}{8}\frac{1+2(l_{NT}/d_{NT})\eta_L V_{NT}}{1-\eta_L V_{NT}} + \frac{5}{8}\frac{1+2\eta_T V_{NT}}{1-\eta_T V_{NT}}\right] \tag{5}$$

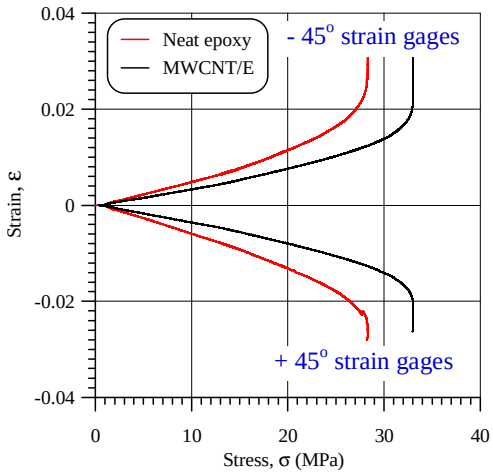

Fig. 9. Stress-strain diagrams of neat epoxy and MWCNT/E nanocomposites in shear tests

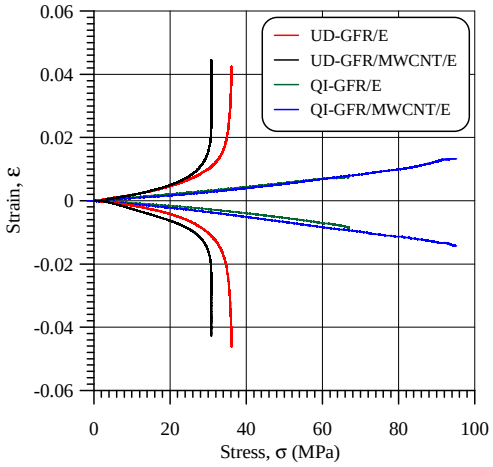

Fig. 10. Stress-strain diagrams of nano-hybridized and control laminates in shear tests

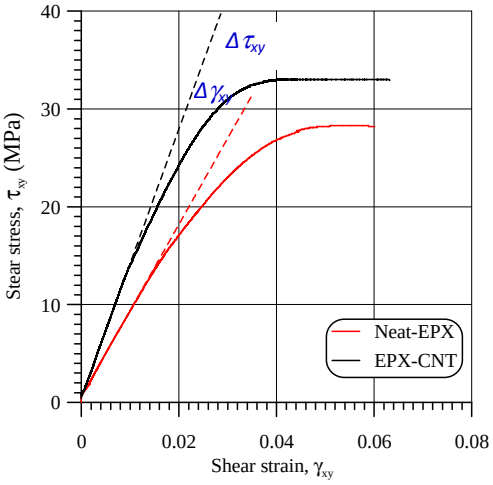

Fig. 11. Shear stress-shear strain diagrams of neat epoxy and MWCNT/E nanocomposites in shear tests

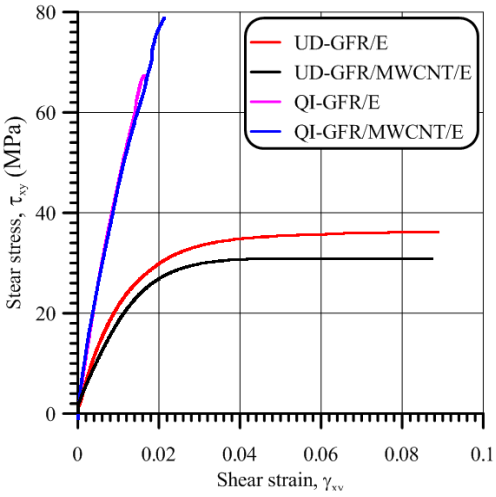

Fig. 12. Shear stress-shear strain diagrams of nano-hybridized and control laminates in shear tests

where *Ec* is the Young's modulus of the composite, E_m is the matrix Young's modulus (=2.247 GPa [1]), E_{NT} is the nanotube Young's modulus (=1 TPa [4,5]), l_{NT} is the average length of the nanotubes (= 30 µm, Table 1), d_{NT} is the average outer diameter of the nanotubes (= 6 nm, Table 1), V_{NT} is the volume fraction of MWCNT in the composite. The values of η_L, η_T, and V_{NT} are calculated from the following equations:

$$\eta_L = \frac{(E_{NT}/E_m)-(d_{NT}/4t_{NT})}{(E_{NT}/E_m)+(l_{NT}/2t_{NT})} \quad (6)$$

$$\eta_T = \frac{(E_{NT}/E_m)-(d_{NT}/4t_{NT})}{(E_{NT}/E_m)+(d_{NT}/2t_{NT})} \quad (7)$$

$$V_{NT} = \left[1+\left(\frac{\rho_{NT}}{\rho_m}\right)\left(\frac{1-M_{NT}}{M_{NT}}\right)\right]^{-1} \quad (8)$$

where M_{NT} is the weight fraction of the MWCNTs (1.0 wt%), ρ_{NT} is the density of the MWCNTs (=2.25 g/cm^3 [5]), ρ_m is the density of polymer matrix (1.103 g/cm^3), and *t* is the thickness of graphite layer (= 0.34 nm) [7,21,36].

The calculated values of η_L, η_T, and V_{NT} are respectively equal 0.00989, 0.9708, and 0.493%. Based on these results the estimated value of Young's modulus of MWCNT/E nanocomposites equal 2.678 GPa.

Based on the isotropy assumption, the shear modulus can be calculated using the following equation, which expresses the relation between tensile and shear moduli [21].

$$G_C = \frac{E_C}{2(1+\nu_C)} \quad (9)$$

where G_C and v are the shear modulus and Poisson's ratio of MWCNTs-nanocomposites respectively. Substituting in the above equation with v_c=0.32, the estimated value of IPSM equal 1.014 GPa. Only, 11% variation is found between the predicted IPSM of MWCNTs-nanocomposite using the above equation and the experimental results (IPSM = 1.141 GPa).

4. CONCLUSIONS

Nanophased epoxy with 1 wt% MWCNT is ultrasonically prepared and used to fabricate MWCNTs-nanocomposite as well as to hybridize advanced composite laminates with different fiber configuration. The sonication conditions are carefully selected based on the extensive literature review. The nano-hybrid composite laminates is fabricated using hand lay–up technique. Applying rolling to the composite laminates using special aluminum roller contributes in removing any visible air bubbles, providing fast impregnation and good wetting of glass fibers with the nanophased epoxy and accordingly, improves the fiber/matrix interfacial bond strength. In additions, applying rolling with moderate pressure played an important role in de–agglomeration of the MWCNTs owing to their high aspect ratio that result in strong attractive forces between the MWCNTs themselves and the van der Waals attractive interactions. Accordingly, most of the investigated materials gain improvements in their mechanical properties.

Scanning electron microscope examination of the MWCNTs-nanocomposite showed that the selected sonication parameters result in a good distribution of MWCNTs in epoxy resin. SEM images of the fractured surfaces of the UD-GFR/MWCNT/E laminate showed that the nanophased matrix appears firmly sticking to the fiber surface owing to the stronger interfacial bond strength compared to the fracture surface of control laminate, which is characterized by clean fibers.

The ultimate IPSS of MWCNTs-nanocomposite has 40.9% improvements compared to neat epoxy. The high improvement in IPSS of MWCNTs-nanocomposite was due to transferring the load (stress) from the low strength matrix to the well dispersed high strength MWCNTs via the strong interface bond strength between them.

The first knee load of QI-GFR/MWCNT/E laminate was characterized by specimen delamination at the contact with loading grips. Because the delamination is a matrix-dominated, the improvement in the first knee IPSS (39.5%) approaching the same improvement level of MWCNTs-nanocomposite (40.9%).

The ultimate IPSS of QI-GFR/MWCNT/E $[0/\pm45/90]_s$ laminates is dominated by the ultimate failure of the different layers. The longitudinal layers with 0° fibers are fiber-dominated and hence, their contribution to the ultimate IPSS improvements is insignificant. Therefore, the improvement in the ultimate IPSS of QI-GFR/MWCNT/E laminate (29.7%) is due to the presence of 90° and ±45° layers, which are dominated respectively by matrix and fiber/matrix interface properties.

The IPSS of UD-GFR/MWCNT/E laminate has insignificant improvement (1.4%). These result because the IPSS of the unidirectional laminate is controlled by the fiber properties.

The IPSM of MWCNTs-nanocomposite improved by 21.9% compared to the neat epoxy. This result is due to transferring the load (stress) from the low modulus matrix (2.247 MPa) to the well dispersed high modulus MWCNTs (1 TPa) via the strong interface bond strength between them. The improvements in the IPSM of nano-hybridized composite laminates are about 17% compared to the control laminates. This result was due to the IPSM of nano-hybridized composite laminates depend on the first linear portion of the shear stress-shear strain curves, which is dominated by the enhancements in fiber/matrix interface properties. The predicted IPS modulus of MWCNT/E agrees very well with the experimental results with only 11% variation.

COMPETING INTERESTS

Author has declared that no competing interests exist.

REFERENCES

1. Alnefaie KA, Aldousari SA, Khashaba UA. New development of self–damping MWCNT composites. Composites: Part A. 2013;52:1-11.
2. Aldousari SM, Hedia HS, Hamed MA, Khashaba UA. Design, manufacture and analysis of composite epoxy material with embedded silicon carbide (SiC) and alumina (Al_2O_3) fibers. Materials Testing. 2015;57:72-84.
3. Aldousari SM, Khashaba UA, Hamed MA, Hedia HS. Design, manufacture and analysis of composite epoxy material with embedded MWCNT fibers. Materials Testing. 2014;56:1029–1041.
4. Montazeri A, Javadpour J, Khavandi A, Tcharkhtchi A, Mohajeri A. Mechanical properties of multi-walled carbon nanotube/epoxy composites. Materials and Design. 2010;31:4202–4208.
5. Lachman N, Wagner HD. Correlation between interfacial molecular structure and mechanics in CNT/epoxy nano–composites. Compos Part A-Appl S. 2010;41:1093–1098.
6. Yang J–P, Chen Z–K, Feng Q–P, Deng Y–H, Li Y, Ni Q–Q, Yu S–Y. Cryogenic mechanical behaviors of carbon nanotube reinforced composites based on modified epoxy by poly(ethersulfone). Compos Part B-Eng. 2012;43:22–26.
7. Loos MR, Yang J, Feke DL, Manas–Zloczower I. Effect of block–copolymer dispersants on properties of carbon nanotube/epoxy systems. Compos Sci Technol. 2012;72:482–488.
8. Falvo MR, Taylor II RM, Helser A, Chi V, Brooks Jr FP, Washburn S, Superfine R. Nanometre–scale rolling and sliding of carbon nanotubes. Nature. 1999;397:236–237.
9. Tanahashi M. Development of fabrication methods of filler/polymer nanocomposites: With focus on simple melt–compounding–based approach without surface modification of nanofillers. J Mater. 2010;3:1593–1619.
10. Montazeri A, Montazeri N. Viscoelastic and mechanical properties of multi walled carbon nanotube/epoxy composites with different nanotube content. Mater Design. 2011;32:2301–2307.
11. Yang S, Lin W, Huang Y, Tien H, Wang J, Ma CM, Li S, Wang Y. Synergetic effects of graphene platelets and carbon nanotubes on the mechanical and thermal properties of epoxy composites. Carbon. 2011;49:793–803.
12. Theodore M, Hosur M, Thomas J, Jeelani S. Influence of functionalization on properties of MWCNT–epoxy nano-composites. Mat Sci Eng A-Struct. 2011;528:1192–1200.
13. Martone A, Formicola C, Giordano M, Zarrelli M. Reinforcement efficiency of multi–walled carbon nanotube/epoxy nano composites. Compos Sci Technol. 2010; 70:1154–1160.
14. Sawi IE, Olivier PA, Demont P, Bougherara H. Investigation of the effect of double–walled carbon nanotubes on the curing reaction kinetics and shear flow of an epoxy resin. J Appl Polym Sci. 2012;126:358–366.
15. Pascault J–P, Williams RJJ. Epoxy polymers new materials and innovations. Wiley–VCH Verlag GmbH & Co. KGaA; 2010.
16. Zhou T, Wang X, Wang T. Cure reaction of multi–walled carbon nanotubes/diglycidyl ether of bisphenol A/2–ethyl–4–methylimidazole (MWCNTs/DGEBA/EMI–2,4) nanocomposites: Effect of carboxylic functionalization of MWCNTs. Polym Int. 2009;58:445–452.
17. Tao K, Yang S, Grunlan JC, Kim Y–S, Dang B, Deng Y, Thomas RL, Wilson BL, Wei X. Effects of carbon nanotube fillers on the curing processes of epoxy resin–based composites. J. Appl Polym Sci. 2006;102:5248–5254.
18. Rodgers RM, Mahfuz H, Rangari VK, Jeelani S, Carlsson L. Tensile response of SiC-Nanoparticles reinforced epoxy composites at room and elevated temperatures. 16th Int. Conf. Composite Materials, Kyoto Japan. 2007;1-6.
19. Khashaba UA. In-plane shear properties of cross-ply laminates with different off-axis angles. J. Composite Structurs. 2004;65: 167-177.
20. Tsai J-L, Wu MD. Organoclay effect on mechanical responses of glass/epoxy nanocomposites. J. Composite Materials. 2008;42:553–568.
21. Kim M, Park Y-B, Okoli OI, Zhang C. Processing, characterization, and modeling

of carbon nanotube-reinforced multiscale composites. Composites Science and Technology. 2009;69:335–342.
22. Zhou X, Shin E, Wang KW, Bakis CE. Interfacial damping characteristics of carbon nanotube–based composites. Compos Sci Technol. 2004;64:2425–2437.
23. Bal S. Experimental study of mechanical and electrical properties of carbon nanofiber/epoxy composites. Mater Design. 2010;31:2406–2413.
24. Khan SU, Li CY, Siddiqui NA, Kim J–K. Vibration damping characteristics of carbon fiber–reinforced composites containing multi–walled carbon nanotubes. Compos Sci Technol. 2011;71:1486–1494.
25. Ayatollahi MR, Shadlou S, Shokrieh MM. Fracture toughness of epoxy/multi–walled carbon nanotube nano–composites under bending and shear loading conditions. Mater Design. 2011;32:2115–2124.
26. Sun L, Warren GL, O'Reilly JY, Everett WN, Lee SM, Davis D, Lagoudas D, Sue H–J. Mechanical properties of surface–Functionalized SWCNT/epoxy composites. Carbon. 2008;46:320–328.
27. Jang J–S, Varischetti J, Lee GW, Suhr J. Experimental and analytical investigation of mechanical damping and CTE of both SiO_2 particle and carbon nanofiber reinforced hybrid epoxy composites. Compos Part A-Appl S. 2011;42:98–103.
28. Uddin MF, Sun CT, Improved dispersion and mechanical properties of hybrid nanocomposites. Compos Sci Technol. 2010;70:223–230.
29. Taurozzi JS, Hackley VA, Wiesner MR. Protocol for the preparation of nanoparticle dispersions from powdered material using ultrasonic disruption. Ceint/Nist Protocol (http://ceint.duke.edu/allprotocols), Ver.1; 2010.
30. Preghenella M, Pegoretti A, Migliaresi C. Thermo–mechanical characterization of fumed silica–epoxy nanocomposites. J Polym. 2005;46:12065–12072.
31. Bittmann B, Haupert F, Schlarb AK. Ultrasonic dispersion of inorganic nanoparticles in epoxy resin. Ultrason Sonochem. 2009;16:622–628.
32. Chen C, Justice RS, Schaefer DW, Baur JW. Highly dispersed nanosilica–epoxy resins with enhanced mechanical properties. Polymer. 2008;49:3805–3815.
33. Zhou Y, Pervin F, Jeelani S, Mallick PK. Improvement in mechanical properties of carbon fabric–epoxy composite using carbon nanofibers. J Mater Process Tech. 2008;198:445–453.
34. Srivastava VK. Modeling and mechanical performance of carbon nanotube/epoxy resin composites. Mater Design. 2012;39: 432–436.
35. Kanagaraj S, Varanda FR, Zhil'tsova TV, Oliveira MSA, Simões JAO. Mechanical properties of high density polyethylene/ carbon nanotube composites. Composites Science and Technology. 2007;67:3071–3077.
36. Gojny FH, Wichmann MHG, Kpke U, Fiedler B, Schulte K. Carbon nanotube-reinforced epoxy-composites: Enhanced stiffness and fracture toughness at low nanotube content. Compos Sci Technol. 2004;64:2363-2371.

Peer-review history:
The peer review history for this paper can be accessed here:
http://sciencedomain.org/review-history/14818